3

Force platform and kinematic analysis

ANDREW A. BIEWENER and ROBERT J. FULL

1. Introduction: forces and motion of rigid bodies

Animals exert forces to move objects in their environment and to move themselves from place to place. Body segment motion, in turn, produces inertial forces that must also be countered by the muscles controlling motion at related joints. Kinetics involves the study of the forces acting on rigid bodies. Kinematics is the study of the motions produced by those forces. Linking the two analyses together, provides a powerful non-invasive approach for studying the biomechanics of animal locomotion, and motor activity in general. For instance, measurements of the forces applied externally to an animal's body (such as ground reaction forces exerted on an animal's limbs when it runs), coupled with kinematic and anatomical data of the limb, allows an analysis of the internal forces that limb muscles must produce to counter externally applied forces. The data obtained from such studies are fundamental to our understanding of how the design of musculoskeletal structures is related to the physical demands placed upon them during various functional activities of the animal in question. In addition, kinematic analysis alone can provide estimates of the inertial loads associated with body segment motion that must be controlled by muscles. Such analyses are particularly important in relation to studies of nervous system control of motor function.

2. Design of force platforms

Force platforms are instruments that record the ground reaction forces exerted by an animal when its limb lands on the platform during the 'support phase' of the stride (*Figure 1*). The following criteria are important to the design of a force platform:

- independent measurement of force in three orthogonal planes
- low 'cross-talk' between force components
- high-frequency response
- linear response over a sufficient range and sensitivity of force measurement

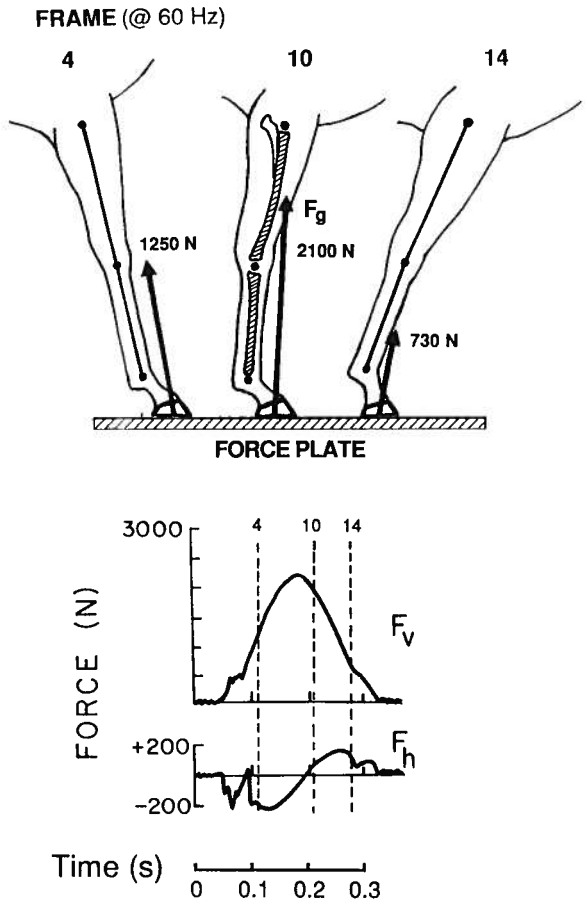

Figure 1. Drawings of the position of the forelimb of a horse in relation to the ground reaction force vector (F_g) at the beginning, middle, and end of the support phase of a fast trot. Below are the records of the vertical (F_v) and horizontal (F_h) components of the ground reaction force measured by the force platform. The film of the animal's limb position is synchronized to the ground reaction force recordings by means of a shutter pulse from the camera's shutter, or by some other timing device (e.g. an LED in parallel with a DC voltage source, such as a battery, that is switched on in the field of the video camera can be used to synchronize video tapes to recorded signals).

- uniform response over the platform's surface
- resolution of the point of application or 'centre of pressure' of the ground reaction force
- proper dimensions of the platform's surface in relation to the animal to be studied

Commercially available force platforms (for example, from AMTI & Kistler Instrument Corp.) are designed generally for use in studies of human gait,

and hence, are rather large in size. Whereas these platforms are appropriate for use in large animal studies (1–3), they are impractical for studies of small animals. In addition, while the performance of commercially available force plates is good, their cost is comparatively high.

Heglund (4) describes a simple approach for the design of a force platform that emulates the performance of commercially available platforms at a fraction of their cost. The construction and specifications of a force platform outlined here follow Heglund's basic design, but include modifications (introduced by N. C. Heglund and R. Blickhan) that facilitate its construction and enable the measurement of force in three directions.

The ground reaction force (F_g) acting on an animal's limb can be resolved into three independent components: vertical (F_z), horizontal (F_x, fore-aft in direction of the animal's travel) and mediolateral (F_y). For species that move their limbs in a para-sagittal plane (for example, cursorial mammals), the mediolateral forces acting on the limb are generally quite small (<5–8%) in relation to the horizontal and vertical ground reaction forces. Consequently, these often can be ignored without incurring significant error in mechanical analyses of the limb. Measurement of only the vertical and horizontal forces also simplifies kinematic analysis of the limb (see below), as films or video recordings need be taken in only a single plane (most commonly in lateral projection). When all three axes are of importance (for example, mediolateral forces are significant in insects and the lateral undulatory locomotion of lizards), three-dimensional analysis of limb movement is required.

Irrespective of whether two or three components of ground reaction force are to be measured, it is essential that the 'cross-talk' between channels be low (typically <3%; see *Protocol 1* below). In addition to minimizing cross-talk, the platform must be designed to have a sufficiently high frequency response (its unloaded natural frequency of vibration) to ensure that the highest frequency components of the ground reaction force that are of interest are faithfully recorded. Generally, the platform's natural frequency should be an order of magnitude greater than the primary signal frequency. In small mammalian species, such as the chipmunk (5), the duration of limb contact at a fast gallop is about 50 msec, corresponding to a primary signal frequency of 10 Hz (stride period: 100 msec). Hence, the natural frequency of the plate should be minimally 100 Hz. To record higher frequency transients in the ground reaction force signal, such as the impact spike present at the start of ground contact of many animals, the frequency response of the force plate must be that much higher.

Obviously, the output of the force platform should be linear in response to applied force in each direction over the full range of forces that are to be measured. Knowing the weight (W) of the animal to be studied, the platform can be designed to measure safely the maximally anticipated load ($10 \times W$ is a safe estimate). A trade-off exists, however, between the range and sensitivity of force measurement. In addition to giving a linear response over an appropriate range of forces, the force platform ideally should be insensitive to where on its

surface the animal's foot lands. Typically, variation due to the position of applied force should be less than 2–3% worst-case (that is, at the extremes of the plate's surface). This can easily be determined in the vertical direction by placing a known load at varying locations on the plate's surface and comparing the output.

A potentially critical source of error in the analysis of individual limb mechanics is the location of the point of application, or centre of pressure, of the ground reaction force (F_g) on the foot. The centre of pressure changes during the support phase, generally progressing anteriorly along the base of the foot to the toes at the end of the support phase. As this can produce large errors in the moments that are calculated to act at joints of the limb, especially when the animal's foot is comparatively long (as in plantigrade and digitigrade species), it is desirable to design the platform with the capability of accurately determining the point of application of F_g.

Finally, the overall size of the plate surface depends on the size of the animal (its foot size, stride length, and spacing between contralateral limbs), as well as on the nature of the force analysis to be carried out. In studies of the mechanics of an individual limb, isolated recordings of ground reaction force exerted on one limb must be made. For studies of the mechanical work of terrestrial locomotion (see Chapter 4), the ground reaction forces of all limbs may be recorded through time for one or (preferably) more complete strides. In this case, the force platform must be sufficiently large to span the animal's entire stride length. For larger species, a series of adjacent force platform elements may be required (6, 7).

Figure 2 shows a schematic drawing of a force platform modified after Heglund's (4) original design. Representative dimensions and performance characteristics of two different sized platforms constructed according to this design are given in *Table 1*. The force transducing elements of the platform consist of two metal beams (front and rear) that support a light-weight, stiff panel which serves as the platform's surface. Honeycomb aluminium panels used in aircraft design (Hexcel Corp.) work well for this purpose; however, cardboard or wood may be used for much smaller animals, such as insects (8). A thin rubber or textured (wall-paper) covering may be applied to a metal panel to provide a non-skid surface for the animal to run over.

The basic design of the platform involves the independent measurement of force in each direction by strain gauges mounted to spring blade elements of the front and rear force beams. Equations of beam-theory are used to calculate the appropriate dimensions of the force beams, according to the mechanical properties of the beam metal, the maximum load limit, and the frequency response of the platform (4). For a maximum applied load (P), blade thickness (h) can be determined according to

$$h = \left[\frac{6PL}{b\,S}\right]^{0.5} \qquad (1)$$

where L is the length of the cantilever formed by the one-half of the blade, b

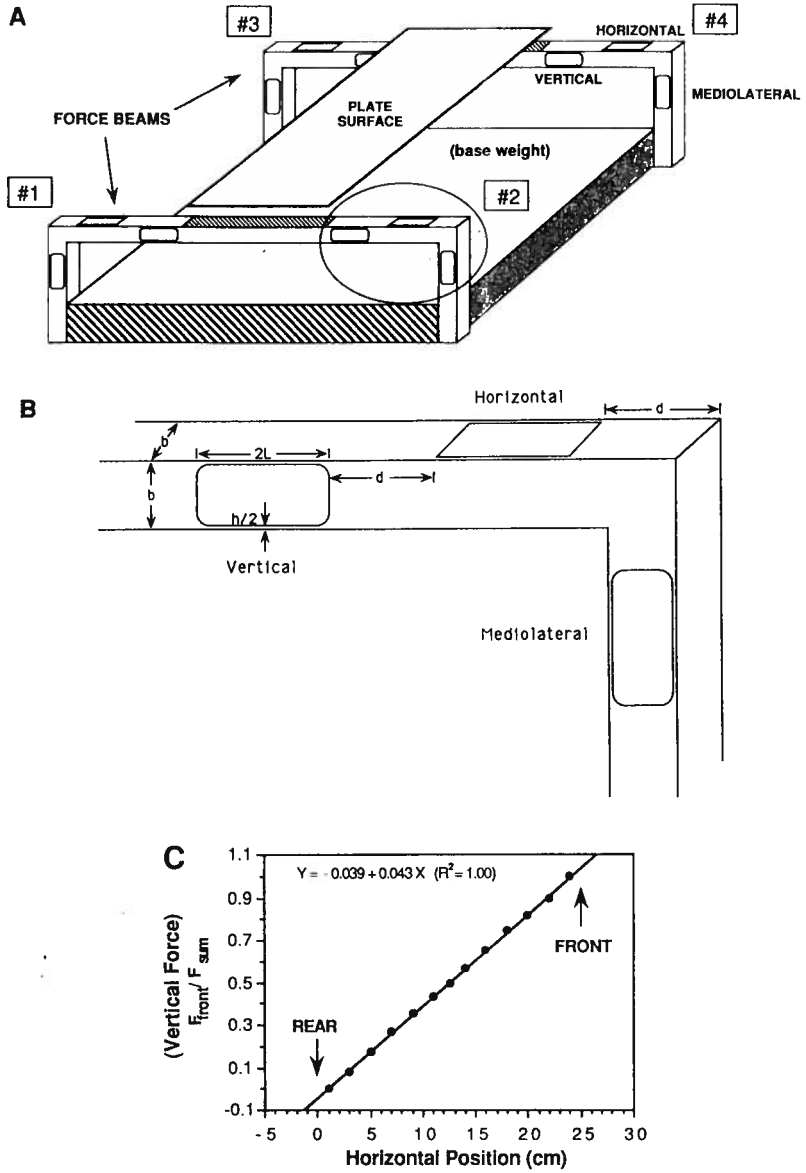

Figure 2. **A**: Schematic drawing of the force platform design. **B**: Enlarged drawing of one set of spring blade elements (vertical, horizontal, and mediolateral) from one beam corner (#2), showing the dimensions which determine the overall sensitivity and performance of the plate, **C**: A representative calibration of horizontal position output based on vertical force (F_{front}/F_{sum}), obtained by placing a known weight at specific locations along the length of the plate.

Table 1. Specifications for representative force platforms

	Plate A	Plate B
Animal weight (*N*)	0.5	20
Peak load, *P* (*N*)	13.5	200
Plate dimensions		
length (m)	0.12	0.30
width (m)	0.06	0.20
Surface thickness (mm)	2.3	9.53
material	aluminium honeycomb panel (Hexcel Corp.)	
Beam material	Brass	Steel
stiffness, E (GPa)	105	200
yield strength (MPa)	105	250
density (kg m^{-3})	1000	7860
Unloaded weight (*N*)	0.247	13.0
Unloaded natural frequency (Hz)	400	200
Beam dimensions		
b (mm)	6.35	18.06
l (mm)	6.00	9.00
h (mm)	0.357	0.735
b/h ratio	17.79	25.91

is the blade width, and S is the yield strength of the beam metal. The ratio b/h should be at least 14 in order to keep the cross-talk between channels to a few per cent. The weight of the suspended portion of the platform relative to the stiffness of the spring blades determines its natural frequency of vibration. The weight of the beams and the plate surface can be calculated based on their density, once their dimensions are known. The self-loaded natural frequency (f_{nat}) of the platform then is

$$f_{nat} = \frac{0.5}{(2D)^{0.5}} \tag{2}$$

where D is the deflection of the plate under these conditions. D can be calculated as

$$D = \frac{4WL^3}{Ebh^3} \tag{3}$$

where W is the suspended weight of the platform and E is the elastic modulus of the beam metal. Because the suspended weight of the beam is greater for more distal spring blade elements (for example, horizontal vs. vertical in *Figure 2*), the blade element furthest from the platform surface will have the lowest frequency response. Accordingly, the force beams should be constructed so that the force component of greatest interest (typically F_v) is positioned nearest to the platform's surface.

A BASIC computer program (PLTDSGN.BAS) is included which calculates the design of force beams constructed of a material of known mechanical

characteristics (elastic modulus, yield strength, and density) according to these equations.

2.1 Strain-gauge and electronic considerations

Either metal foil or semiconductor strain-gauges may be used to transduce force based on deflections of the spring blade elements. The former are less sensitive (lower voltage output per strain), but have greater temperature stability and are easier to work with. An oven-cured epoxy (for example AE-15, Micromeasurements, Inc.) should be used to bond the gauges to the spring blade elements of the metal beam. Heavy duty spring paper clamps work well for clamping the gauges to the beams. The gauges should be clamped during the curing process to ensure a reliable bond. Accurate alignment of the gauges parallel with the blade axis is important for achieving a uniform response from all blade elements. Lead wires from the strain-gauges should be soldered to insulated lead wires via a strain relief connector mounted adjacent to each strain-gauge.

The strain-gauge leads should be configured as a full-bridge (*Figure 3*) for input to a conditioning Wheatstone bridge amplifier (for example, Vishay model 2120, Micromeasurements). Strain gauges of the horizontal and mediolateral force spring elements each should be grouped into a single channel full bridge circuit. To enable determination of the point of application of the ground reaction force in the plane of the animal's motion, however, the vertical force strain-gauges of the front and rear beams should be wired separately as two full-bridge circuits (*Figure 3*), providing independent vertical force measurement at the front and rear of the plate. For uniformity and accuracy, the outputs of the front and rear vertical channels must be the same. This can be achieved by varying the gain of each bridge amplifier channel to give an equivalent output for a load applied at the same relative position to either beam (that is, at the centre of the plate, or at a distance of 10 mm, 20 mm, etc., from either beam).

The voltage outputs of the front vertical, rear vertical, horizontal, and mediolateral channels can be digitally sampled and stored on disk by a computer for subsequent analysis and synchronization with limb coordinate data. Total vertical force is determined by summing the outputs of the front and rear vertical forces in software. The point of force application is then determined by dividing the output of either the front or rear vertical force by the total vertical force. This gives a linear output for position of force application along the length of the plate that is independent of the magnitude of applied force (*Figure 2C*). Resolution of position to within ±0.5 mm is possible.

2.2 Force plate calibration

The force plate should be calibrated on a regular basis to check the integrity of the strain-gauges, the electronic circuits and for any changes in sensitivity that may have occurred during its use in previous experiments. *Protocol 1*

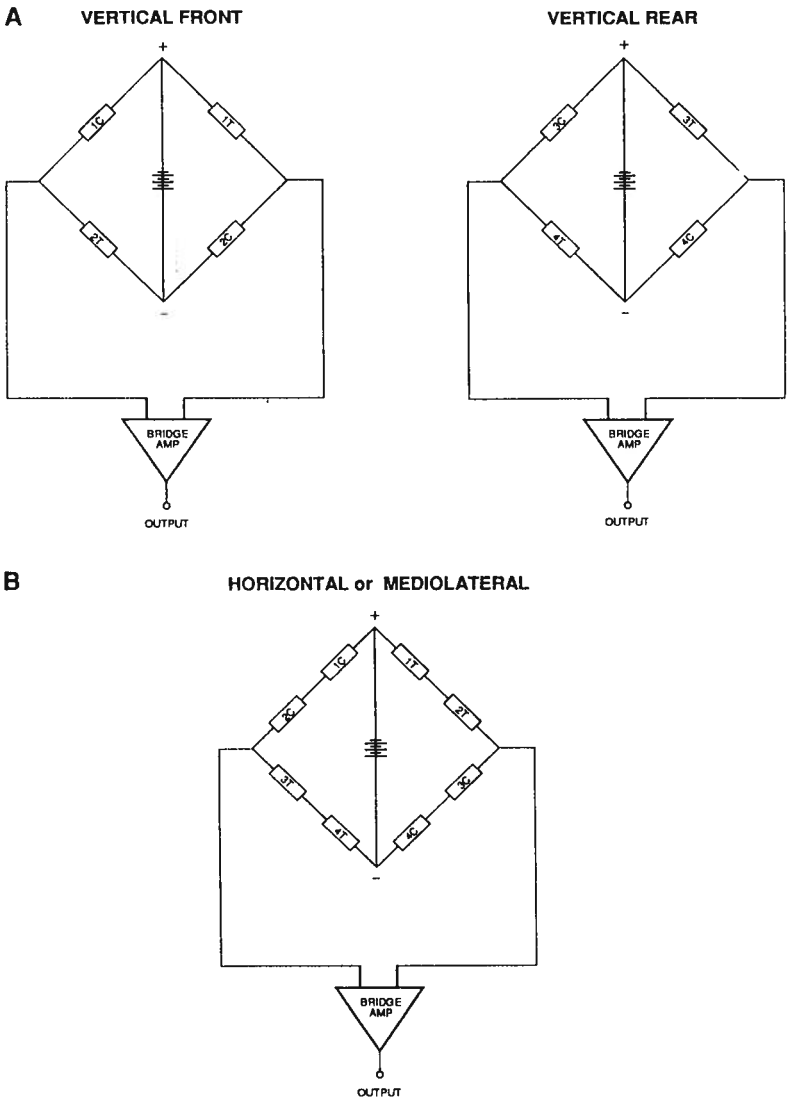

Figure 3. Force platform strain gauge bridge configurations. **A**: Vertical force is transduced as independent full bridges at the front and rear beams of the plate to enable determination of the position of force application along the plate's length (position 0 to 25 cm in *Figure 2C*; see text for details). Strain-gauges are numbered corresponding to *Figure 2* (1C, IT, 2C, 2T, etc.). For three-dimensional analyses of the limb, if pairs of strain-gauges (C and T) are configured as four independent half-bridges for each corner of the plate, the centre of pressure of the ground force can be determined at any point on the plate. **B**: Horizontal (fore-aft) and mediolateral forces are each configured as a single full bridge circuit, summing these forces over the entire plate.

outlines a complete calibration and testing of the force plate's performance characteristics. The following supplies are needed:

- metric ruler
- digital voltmeter
- calibrated set of weights (total weight being greater than the maximum expected force that is to be recorded)
- frictionless pulley and cable or force transducer and protractor

---

Protocol 1. Calibration procedures

1. Mark off the length and width of the plate at known intervals (say, millimetres or centimetres).
2. Place a weight, equal to or greater than the maximum expected force that is to be recorded, in the centre of the force plate and adjust the gain of the front and rear vertical force amplifier channels to give the same voltage output. Check the uniformity of the front and rear vertical force outputs again at 50% of this weight.
3. To calibrate vertical force, record the front and rear vertical force outputs using a digital voltmeter (the sum of these equals total vertical force, F_v) as known increments in weight are applied to the centre of the plate.
4. To calibrate horizontal and mediolateral force, two approaches can be used: (a) a cable (silk suture, nylon cord, etc.) is taped to the plate's surface, passed over a frictionless (air) pulley positioned at the same height as the force plate and known increments of weight are attached to the cable's free end; or (b) the cable is attached to a calibrated force transducer and pulled on by the experimenter, with the angle of force relative to horizontal determined by the protractor. The applied horizontal or mediolateral force is the cosine of the angle times the force measured by the transducer.
5. Sensitivity of the force plate to positional variation in the location of applied force is determined by applying a uniform weight to different locations on the plate's surface and recording the summed output of the front and rear vertical force channels.
6. Cross-talk is determined by recording the horizontal and mediolateral force outputs when a known force is applied in the vertical direction (following this with the same procedure in the other two directions).[a]
7. Position (or the 'centre of pressure') of force application is determined by placing a uniform weight at known intervals along the length (and width, if two-dimensional positional information is needed) of the plate and recording the separate outputs of the front vertical and rear vertical channels using a digital voltmeter. A position calibration curve (*Figure 2C*) is then constructed by dividing either the front or rear vertical force output by the total vertical force.[b]

Protocol 1. *Continued*

8. The natural frequency (f_{nat}) of the force plate can be determined by lightly striking the platform with a metal object, causing the force platform to 'ring'. The voltage signal of the force platform in each direction displayed on an oscilloscope or computer monitor will show this high-frequency ringing ($=f_{nat}$) superimposed on the primary force signal.

[a] An approximate correction for cross-talk can be achieved by determining the cross-talk between vertical, horizontal, and mediolateral directions at various locations mapped out over the plate's surface. The magnitude of force in each direction due to cross-talk from the opposite two directions can then be subtracted from recorded force signals in software for the various locations on the plate's surface (8).

[b] A convenient way to check the position calibration of the plate is to videotape a ball that is rolled over the plate's length (the weight of the ball will depend on the sensitivity range of the force plate). From these data the centre of pressure is easily determined from the tape.

---

3. Kinematic analysis

Kinematics is the description of the motion of rigid bodies independent of the forces that generate their movement. The following parameters are important for kinematic analysis:

- coordinate system set-up
- image acquisition
- data analysis

3.1 Coordinate system

The first step in kinematic analysis is to decide on the motion of interest. If the motion occurs in a single plane, then a two-dimensional coordinate system (for example, x, y) may be sufficient. If the motion of interest involves two planes, then a three-dimensional coordinate system (for example, x, y, z) must be used. The origin must be located in the appropriate reference frame. If the motion of an animal relative to the ground is important, then the coordinate system should be located with respect to landmarks on the ground. If the motion of an appendage is to be described relative to the movement of the body, then the coordinate system should be located with respect to points on the body (for example, origin at the body's centre of mass). Angles must be defined relative to a zero reference coordinate and should be designated as positive when they change clockwise or counter-clockwise depending on the direction of movement. Fifteen variables can be required to completely describe the movement of a body or body segment [i.e. position of the segment's centre of mass (x, y, z), linear velocity (x, y, z), linear acceleration (x, y, z), angle in two planes (θ_{xy}, θ_{yz}), angular velocity (ω_{xy}, ω_{yz}) and angular acceleration (α_{xy}, α_{yz}); see Winter (9)].

3.2 Image acquisition

Once the coordinate system of the motion has been established, a decision must be made as to the method of image acquisition. A major source of potential error lies in the rate at which images are captured (that is, sampling rate). Sampling theory demands that images must be captured at a minimum of twice the frequency of the motion's highest frequency component. In practice, a tenfold greater sampling rate is usually minimal if frequency and amplitude of motion are to be reliably described. Aliasing errors occur if the sampling frequency is too low (*Figure 4*). These errors can produce a completely false description of motion by generating signals of various frequencies that differ from the frequency of the signal of interest. Higher sampling rates (that is, greater than ten times the motion frequency of interest) are recommended if position data are to be used to determine velocity and acceleration. Small errors in position (phase or amplitude) can lead to enormous errors in velocity and acceleration when position is differentiated directly. Noise is a second reason why sampling rates should not be too low. If the sampling rate is sufficiently high, motion noise can be characterized and later removed (see data analysis). If the frequency of the signal of interest is unknown, then it is preferable to capture the motion at a high frequency initially so that a spectral analysis can be undertaken to determine the frequencies that contribute the most to the signal power. This procedure also helps to identify the frequency range of signal noise, often composed of high frequencies, which can be subsequently removed prior to data analysis. After determining the sampling frequency required, a decision can be made as to which image capture system is most appropriate.

3.2.1 Image sampling rate and video cameras

At present, the method of choice for image acquisition is videography (see ref. 10 as a general reference). In the future, the standard is likely to be direct capture of images in computer memory (for example, the Kodak EMS system). A standard video camera (for example, Panasonic model PV series) captures 60 images or 'fields' per second. Each field is composed of 262.5 video scan lines (Standard VHS, NTSC system; 400 lines for Super VHS). Standard playback of a video tape takes two fields and interlaces them to generate a single frame (1 frame = 2 fields). A frame is composed of 525 lines (a composite of two fields captured at 1/60th of second apart) and has a frequency of 30 Hz. Standard frames must be separated into fields to attain a recording frequency of 60 Hz. Video frame grabber computer boards capture a frame and can separate it into two fields. Motion analysis systems (such as from Peak Performance Technologies, Inc.) can use the single fields for analyses.

Higher sampling rates can be attained by video cameras (for example, Kodak EktaPro and NAC-400) that split the fields into multiple pictures.

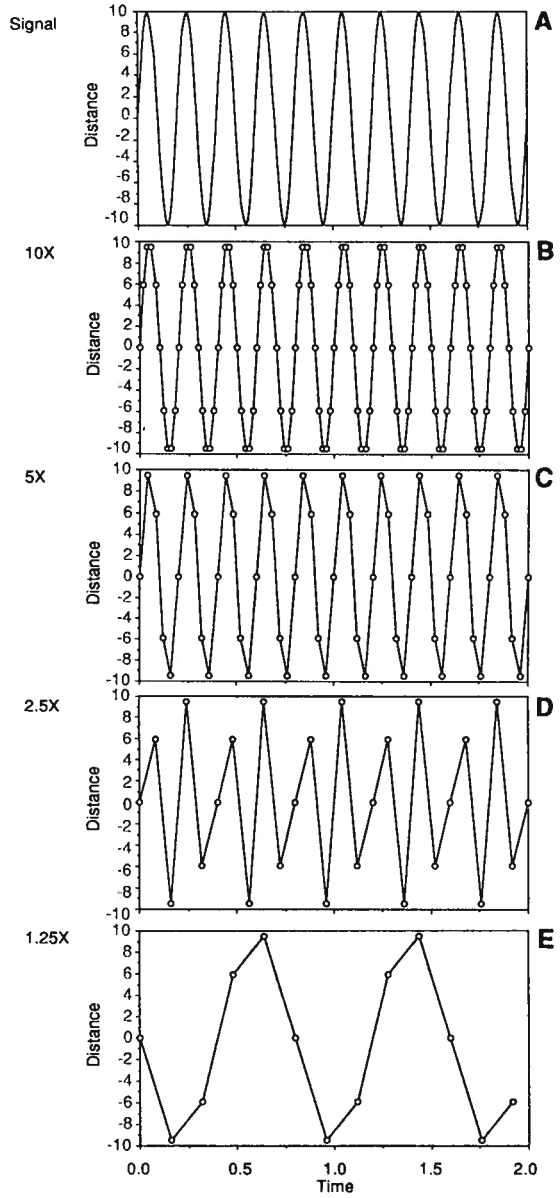

Figure 4. Sample rate/aliasing example. **A**: True signal of an object's motion. **B**: Description of motion for sampling rate of 10 times the frequency of the signal; **C**: 5 times the frequency of the signal; **D**: 2.5 times the frequency of the signal; and **E**: 1.25 times the frequency of the signal. Major signal distortion is apparent at 5 times the true frequency and would result in large errors in velocity and acceleration. Lower sampling frequencies completely distort the signal.

Again, it is important to be certain whether the image that you are analysing is a frame, field, or picture (1 frame = 2 fields; 1 field = 1 to 6 pictures). For example, a sampling rate of 120 Hz is attained by splitting a field into two pictures each taken 1/120th of a second apart. As with a standard camera, playback of this image on a standard recorder would show one frame composed of two interlaced fields. Each field would contain not one, but two pictures, usually one below the other. This technique has the advantage of increasing imaging capturing rate, but has the disadvantage of decreasing resolution (usually vertical). Splitting fields in two (120 Hz sampling rate) decreases resolution by 50%, whereas splitting fields into 5 pictures (300 Hz sampling rate) decreases resolution by 80%.

The highest sampling rates (200–6000 pictures/sec) are attained by rapidly moving the video tape during recording (for example, Kodak EktaPro; NAC-400). These systems allow playback directly on standard recorders or downloading to standard systems. However, in some cases a time base correction (that is, sending the signal through a time-base corrector) is required before the field can be captured by the frame grabber board.

To obtain the least blurred image possible it is often desirable to use a strobe light or a mechanical/electronic shutter. Neither system alters the sampling rate, but each can shorten the exposure time of the picture at a given sampling rate, thus helping to 'freeze' the object. Mechanical/electronic shutters on camera lenses are often adjustable so that several different exposure times can be selected (e.g. 1/250–1/10 000 sec).

3.2.2 Calibration, lighting, and contrast

Once a camera is selected, its aspect ratio should be determined. Each video camera and lens has a unique ratio of height to width. Video taping a large square of known dimensions is the simplest way to determine this ratio. This correction needs to be made only once for a given camera and lens.

If the motion of interest is confined to one plane, one camera can be used for two-dimensional analysis. The camera should be positioned perpendicular to the plane of motion. Ideally, it should be placed at the height of the subject of interest and levelled. The camera should be placed as far away from the subject as possible to minimize parallax errors. The image should be made as large as possible by increasing the focal length of the lens. This is best accomplished by using a zoom lens with a variable focal length (video cameras either have zoom capabilities or allow a standard C-mount lens to be added). Standard zoom lenses are sufficient for most applications. Lenses that allow greater amounts of light to enter are preferred (that is, low *f*-stops should be used), as high-speed or shuttered cameras typically require more light. A wide open aperture, however, limits the depth of field in which a focused image can be seen; often requiring that a compromise be made between depth of field and exposure time. External lights should be set up to provide the best contrast possible between the subject and the background. In general, the low

light levels and heat transmission associated with video recording is a major advantage compared to the considerably greater lighting intensity required for high-speed light cinematography.

After the system is set up, a scale bar of known length should be video taped in the appropriate plane. The scaling factor for the image can be determined from the bar. The bar should fill as much of the screen as possible. A new scale bar should be video taped if the camera is moved or the focal length is changed.

If the motion of interest occurs in two planes, a three-dimensional kinematic analysis is required. A three-dimensional description of motion can be obtained by using mirrors or by using more than one video camera simultaneously. If a mirror is used, it should be positioned at an angle of 45 degrees to the camera's optical axis to give a perpendicular view to that of the camera. The disadvantage of using only one camera and mirrors is the loss in resolution caused by having two or three images contained on a single field. Since the distance of the subject and image in the mirror differ with respect to the camera, focusing may also be a problem. If two cameras are used, they should be placed at approximately right angles to the field of view. A calibration cube or other shape of known dimensions must be video taped in the same location by both cameras. The calibration shape should again fill the screen and must include a minimum of 6 non-coplanar points that can be seen by both cameras (more points are recommended for direct linear transformation; see data analysis, Section 3.3 below). If two or more cameras are used they should be field synchronized (i.e. 'genlocked'). This can be achieved by signalling a common event in the field of view (for example, a light flash), or by using a SMPTE time code generator that writes the time on the video tape.

In many cases, markers (such as tape, paint, or LEDs) on the subject greatly facilitates digitizing. Markers should provide the greatest contrast possible between the mark and the surrounding background. If the markers are of sufficient contrast, some motion analysis systems have the capacity for auto-digitizing. Remember that markers placed on movable objects, such as clothes or skin, can shift relative to the skeleton as the subject moves.

3.3 Data analysis

After the desired image is captured, the motion of interest must be acquired from the video tape. A video taped frame is acquired by a 'frame-grabber' board which resides in the computer (for example, Data Translation, Matrox). A frame-grabber board converts the analogue video signal to a digital representation of the picture. The digital picture is composed of spots of light or 'pixels' that vary in shades from black (0) to white (256). The board has the capacity to separate a frame into two fields. One or more fields can be stored in the board's memory buffer, while the one field is converted back to analogue and sent to a monitor for digitizing. Digitizing is usually accomplished manually

by super-imposing a cursor over the picture displayed on the video monitor, locating the point of interest with a mouse, and pressing a mouse button to enter the coordinates into computer memory.

Resolution of the motion of interest is dependent upon the number of pixels that the camera sensor possesses (for example, 286 000 pixels for a standard CCD camera), the number of pixels that are captured and generated by the frame grabber board (for example, 512 × 512), and the number of pixels that can be digitized (for example, 1000 × 1000 ½ pixel precision for Peak Performance Tech., Inc.—the Peak system can average position between adjacent pixels identified by the digitizing cursor, each cursor 'point' being a pair of pixels, thereby achieving a resolution that is twofold greater than the frame grabber board). Pixel numbers ranging from 500 to 1000 yield 0.1–0.2% resolution.

Video controller boards can be used to advance the VCR to the next frame or to find specific frames for continued or additional digitizing. Video controller boards also allow the computer to run the recorder (for example, stop, pause, play, rewind, fast forward). A specific frame can be located by the time code on one of the tape's audio tracks (typically channel 2).

Motion analysis systems (Peak Performance Tech., Inc. and Motion Analysis, Inc.) may possess the capacity for auto-digitizing or tracking. High-contrast markers (such as reflective paint, tape, light-emitting diodes, or dark spots) attached to points of interest on the subject are automatically tracked in software. Tracking is accomplished by first identifying the markers or spots by edge detection (comparison of pixel grey level value with a threshold until an outline is achieved) and then calculating their centres (centroid computation). Prediction of the markers' positions in the subsequent field is done by fitting a function (for example, cubic spline) to the previous coordinate data. Software then performs a search for the next marker or spot position. Data capture is far more rapid than by manual digitizing because frame grabber boards can capture multiple frames for analysis. Auto-tracking can save many hours on large projects. Two problems can occur with this method, however: markers may not be located by the software, or they may 'collide' with one another producing tracking errors. Some motion analysis systems (for example, Peak Performance Tech., Inc.) have error checking routines that identify these problems and allow rapid editing or manual digitizing.

3.3.1 2-D analysis

Analysis of movement in two dimensions is accomplished by placing a coordinate system (x, y) onto the field captured by the frame grabber board. The origin of the coordinate system can be digitized as a reference point in every field. This not only corrects for camera motion, alignment, and jitter, but also allows the origin to be placed on a moving object so that relative motion can be determined. Lateral tilt of the camera can be corrected if two reference points (0,0 and x_1,0) are used in every field. To increase the speed

and ease of manual digitizing, some motion analysis software uses point prediction. The cursor can be placed very near the next point to be digitized by applying a curve-fitting function (for example, cubic spline). Once the position data for a trial have been digitized, the velocity and acceleration of these points can be calculated, but not usually before noise reduction (see data filtering, Section 3.4 below).

3.3.3 3-D analysis

Analysis of three-dimensional movement can be accomplished by direct linear transformation (DLT) from data captured on two or more views or cameras (11, 12). The three-dimensional coordinates of a moving object (x, y, z) can be determined from the two-dimensional coordinates (U, V) that are captured by each camera (*Figure 5*). The position of the object (x, y, z) at any

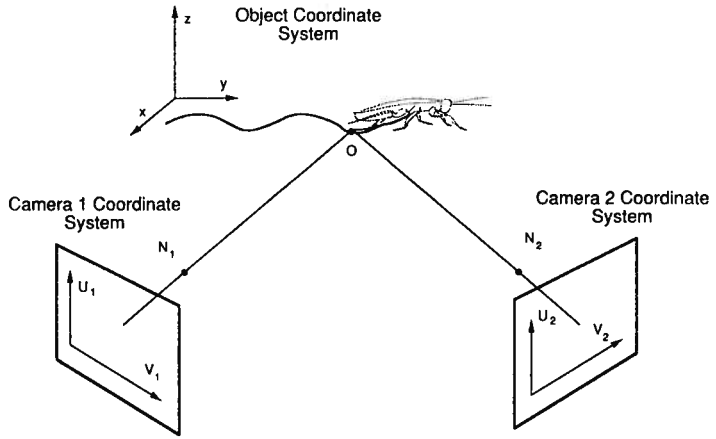

Figure 5. Direct linear transformation of two independent sets of two-dimensional coordinates (U_1, V_1 and U_2, V_2) obtained from two video cameras to three-dimensional coordinates (x,y,z). x, y, z coordinates are related to the camera coordinates by the line ON_1.

instant is directly related to a specific set of camera coordinates (U_1,V_1 and U_2,V_2) by a line or ray that intersects the object (for example, segment ON_1; *Figure 5*). The camera coordinates are related to the object coordinates by the expressions:

$$U = \frac{Ax + By + Cz + D}{Ix + Jy + Kz + 1}$$

$$V = \frac{Ex + Fy + Gz + H}{Ix + Jy + Kz + 1} \qquad (4) \text{ and } (5)$$

where coefficients A through K represent constants which depend on the location of the cameras relative to the object. The values for the 11 co-

efficients can be determined if 6 or more non-coplanar control or calibration points are measured initially. Once the values for the constants are known, digitized points from the two-dimensional camera coordinates can be used to calculate the three-dimensional object coordinates (x, y, z). There are no specific limitations on camera placement when using this method which makes it convenient due to constraints frequently encountered in many experimental set-ups. However, error increases as the angle(s) between the cameras deviate from 90 degrees. Also, it is important to note that lens distortion may increase error significantly when determining 3-D kinematics. Corrections for various type of lens distortion (for example, linear, barrel, pin-cushion) can be incorporated in the DLT as additional coefficients.

3.4 Noise reduction

Raw kinematic data always contain noise due to camera vibrations, videotape imperfections and digitizing inaccuracies. These errors may be small if only position data are required, but can be enormous if the position data are used to determine velocity and acceleration. This results from the fact that differentiated noise increases linearly with frequency. Several techniques have been used to reduce noise. These include:

- Chebyshev least-squares polynomial curve fitting of displacement data followed by polynomial differentiation (13)
- second-order finite difference (14)
- spline function curve-fitting
- digital filtering followed by finite difference techniques (15)

A variety of noise-reduction techniques should be tried by investigators on their particular data sets. Previous comparisons of the filtering techniques have been undertaken. Zernicke *et al.* (16) found that orthogonal polynomial fits tend to over-smooth data compared to cubic spline fits. Pezzack *et al.* (17) found similar results for polynomials up to the 16th degree. Second-order finite difference differentiation tends not to smooth the data enough and results in noisy acceleration data (17). Digital filtering followed by first-order finite difference techniques often provides satisfactory signals (15, 17).

A fourth order, zero-lag Butterworth digital filter is a fast, general purpose filter (9). The filter allows selective rejection of frequencies above or below a given frequency (this is the cut-off frequency, f_c). In most cases, a low-pass filter which attenuates high frequencies is used, because noise is usually of high frequency. The filter sums weighted adjacent raw data and previously filtered data according to the following equation:

$$F_{(i)} = a_1 F_{(i-2)} + a_2 F_{(i-1)} + a_3 R_{(i)} + a_4 R_{(i+1)} + a_5 R_{(i+2)} \qquad (6)$$

where $F_{(i)}$ is a filtered value, $R_{(i)}$ is a raw value, a_x are filter coefficients, and i is the current picture number. The coefficients are determined from the ratio of the sampling frequency to the cut-off frequency.

Filtering can introduce a phase shift in the filtered data. This can be eliminated, however, by filtering the data in the forward direction ($i = 1$ to the total number of pictures) and then in the reverse direction (last picture to $i = 1$). By adopting this procedure, use of the above equation (6) produces a fourth order, zero-lag digital filter.

Selection of an appropriate cut-off frequency is important. The signal near the cut-off frequency is always slightly attenuated depending on the 'steepness' of the filter (that is, how sharp is the filter cut-off). Therefore, if the cut-off frequency is too low with respect to the signal frequency range of interest, signal distortion will occur. On the other hand, if the cut-off frequency is too high, too much noise may pass through the filter. Residual analysis provides an objective method to determine an appropriate cut-off frequency (9). By using a computer, a raw signal can be filtered at a range of cut-off frequencies. The residual (RS) at a given cut-off frequency can be calculated by:

$$RS(f_c) = \left[\frac{1}{N}\sum_{i=1}^{N}(Y_{ri} - Y_{fi})^2\right]^{1/2} \qquad (7)$$

where Y_{ri} is the ith raw data point, Y_{fi} is the filtered data point and N is the sample size. If RS is plotted as a function of f_c, the degree of noise versus signal distortion can be evaluated (*Figure 6*). The area above the segment **ae** and below the horizontal intercept line represents the noise residual. The intercept of the segment (**de**, extended to **a**) is the residual mean square error and is the mean noise for the raw data set. If the sampled data contain no

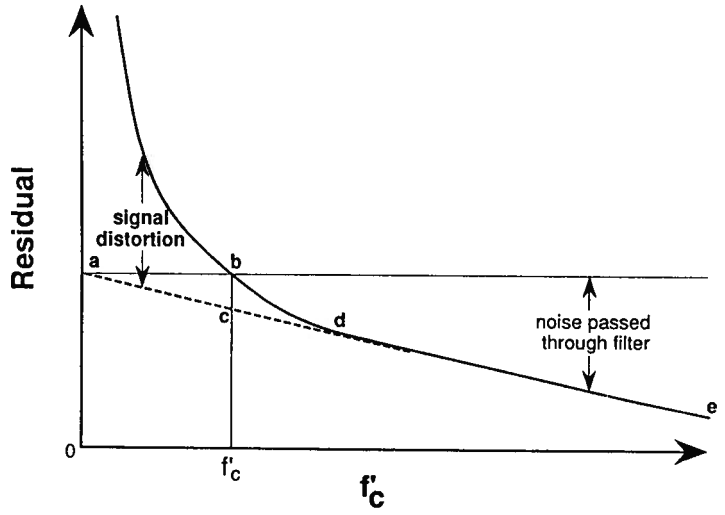

Figure 6. Residual analysis for the determination of an appropriate filter cut-off frequency. Frequency f_c' is the frequency that balances the amount of noise versus signal distortion. See text for details.

signal, just random noise, the residual plot would be a straight line decreasing from an intercept on the ordinate at 0 Hz to an intercept on the abscissa at the Nyquist frequency (0.5 times the sampling frequency). Signal distortion is shown by the steep rise in the residual as the cut-off frequency is decreased (below f_c'). From this graph, one can select the amount of noise and signal distortion that is acceptable. A reasonable selection would be to balance the amount of noise and signal distortion. The noise and signal distortion become equal at the cut-off frequency where the horizontal intercept line intersects the residual function (that is, point **b**). The equality or balance is shown by the fact that segment **bc** represents both the residual noise and signal distortion.

3.5 Velocity calculations

Linear and angular velocities can be determined by using a fourth-order central difference calculation:

$$V_{(i)} = (F_{(i-2)} - 8\,F_{(i-1)} + 8\,F_{(i+1)} - F_{(i+2)})/(12\,\Delta t) \qquad (8)$$

where $V_{(i)}$ is a velocity value, $F_{(i)}$ is a filtered position value, i is the current picture number and Δt is the time difference between pictures. The advantage of this calculation over the simple calculation of average velocity is an improved precision that is achieved by determining the instantaneous velocity at picture i, using the position values both before ($i - 1$, $i - 2$) and after ($i + 1$, $i + 2$). Acceleration can be determined in a similar manner by using a first- and second-order central difference (14).

4. Integrating force and kinematic data: linked segment, free-body analysis

By combining ground reaction force data obtained from a force plate with joint coordinate data obtained from a video analysis system, a free-body analysis (*Figure 7*) can be carried out to calculate joint moments, muscle forces, and bone and tendon stresses (or strains; see also Chapter 6). The limb is treated as a series of rigid segments that are linked together by frictionless pivots (the joints) having from 1 to 3 degrees of freedom of movement (for a planar analysis, only 1 degree of freedom of motion is assumed). For each joint of interest, the moment exerted at the joint at a given instant in time must be calculated. The joint moment is the sum of three components: (i) external moment, (ii) inertial moment, and (iii) gravitational moment. The external moment produced by the ground reaction force is simply

$$M_{ext} = F_g \times R \qquad (9)$$

where R is the orthogonal distance from the vector of ground force to the rotational axis of the joint. The rotational axis of a joint is best determined by

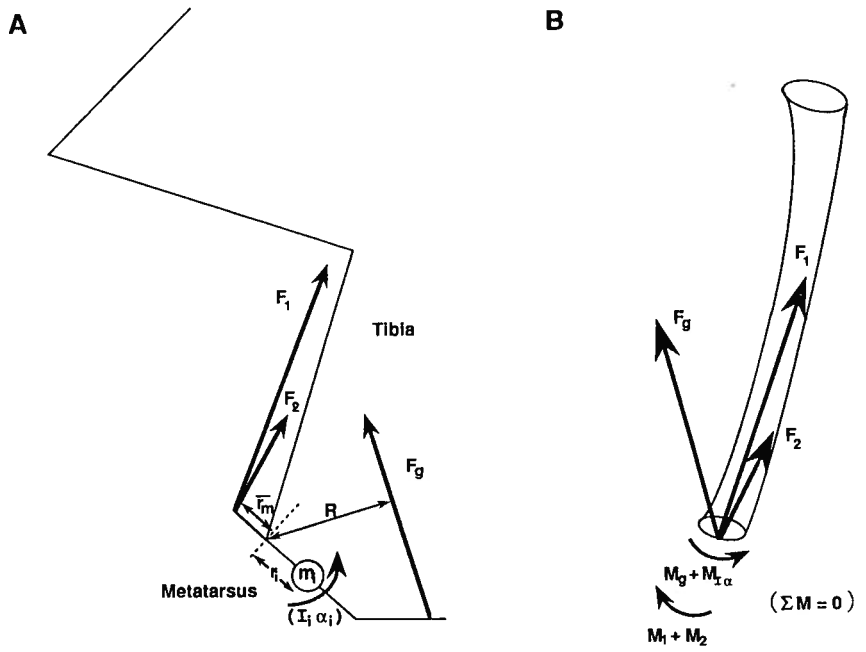

Figure 7. **A**: Schematic drawing of a limb showing the external forces that act on the tibia at a specific time during the support phase of the stride (F_g: ground reaction force; F_1 and F_2: muscle forces). In addition to the moment exerted by the ground reaction force (M_{ext}), the muscles must also counteract the moment of the metatarsus due to its inertia (I_i) and angular acceleration (α_i). During most of the support phase, the inertial moment (M_{inert}) is small compared to M_{ext}. **B**: Free body diagram of the tibia showing the external forces acting on the tibia. Equal and opposite forces (not shown) act to compress and bend the bone, satisfying the conditions of static equilibrium ($\Sigma F = 0$ and $\Sigma M = 0$).

taking a series of radiographs with the joint held in different positions (three is usually sufficient for motion in a single plane) over its functional range of motion. For a three-dimensional analysis, radiographs must be taken with the joint rotated in a second plane (non-coplanar). The intersection of the axes of articulating segments at each joint angle identifies the joint's centre of rotation. This can also be done at the limb surface but is less satisfactory. Markers should be positioned on the overlying skin. The external moment can be decomposed into its component vectors as $M_x = F_x \cdot x$; $M_y = F_y \cdot y$; and $M_z = F_z \cdot z$, where F_x, F_y, and F_z are the components of the ground reaction force and x, y, and z are the respective distances of these components to the joint's centre of rotation.

The inertial moment generated due to the motion of limb segments is

$$M_{inert} = \sum_{i=1}^{n} I_i + m_i r_i^2 \alpha_i \qquad (10)$$

where n is the number of segments distal to the joint of interest, I is the moment of inertia of each segment about its own centre of gravity axis, m is the mass of each segment, r is the distance of the centre of gravity of each segment to the joint's centre of rotation, and α is the angular acceleration ($rad\,s^{-2}$) of each joint segment. These are summed for all segments distal to the joint, with the rotational acceleration of each distal segment measured *relative* to the proximal articulating joint segment (see Chapter 4, Section 3, and refs. 9 and 18 for further details). Gravitational moments due to the weight of each segment are determined as

$$M_{grav} = \sum_{i=1}^{n} m_i\, g\, x_i \qquad (11)$$

where g is gravitational acceleration ($9.81\,m\,s^{-2}$) and x_i is the horizontal distance of the centre of mass of each segment to the joint's centre of rotation. The net total joint moment then is

$$M_{tot} = M_{ext} + M_{inert} + M_{grav}. \qquad (12)$$

During the support phase of an animal's stride, the moments produced by segment inertia particularly at more distal joints, as well as those due to gravity, are typically quite small in relation to those exerted by the ground reaction force and hence, can often be ignored with little error incurred. However, if the animal's limb segments are a large fraction of its total body mass, as in humans, errors incorporated by ignoring segment inertia can be significant, being increasingly large at more proximal joints (19). Schneider and Zernicke (20) give a detailed mathematical description of intersegmental dynamics for a human limb and a FORTRAN subroutine that can be adopted for calculating the component joint moments in the local plane of the articulating segments.

The magnitude of muscle force required to counter the joint's moment is determined by satisfying the condition of static rotational equilibrium (in which the net moment = 0) at a given instant in time

$$F_{muscle} \cdot \bar{r}_m + M_{tot} = 0$$

or

$$F_{muscle} = -M_{tot}/\bar{r}_m \qquad (13)$$

where $\bar{r}_m$ is the weighted mean moment arm of the muscles that are active to counter the moment at the joint. For relatively simple joints, in which only a single muscle is active to counter the joint moment or all muscles have nearly the same line of action and moment arm at the joint (such as the ankle or elbow joint of mammals), $\bar{r}_m$ is easy to determine. It is simply the orthogonal distance from the muscle's line of action to the joint's centre of rotation, which can be determined from dissection and radiographic measurements (see above). These joints are considered to be statically determinant. How-

ever, many joints (e.g. knee, hip, or shoulder of mammals) that are controlled by muscles possessing differing lines of action and moment arms are statically indeterminant. For these joints, no exact solution exists for how muscle force is partitioned between agonist muscles, making it difficult to estimate the moment arm or mechanical advantage of the muscles as a group. In some cases direct *in vivo* recordings of muscle forces (see Chapter 6) can provide an experimental means for quantifying the contribution of individual muscles to total agonist muscle force.

Various optimization criteria and methods can be used to solve for the distribution of muscle force through time among individual muscles acting about an otherwise indeterminant joint (see ref. 21, for example). These approaches use either some quantification of the intensity of muscle electrical activity (EMG; see Chapter 8) or calculate the distribution of muscle forces based on one or more criteria, such as minimizing muscle power output or peak muscle stress. Recently, computational methods based on optimal control strategy have also been developed to tackle this problem (22). In this case, iterative solutions are obtained for the distribution of muscle forces that maximize a certain global criterion (such as maximum jump height). Following Alexander (23), we (24) have made the assumption that the force and hence, the distributed weighting of a muscle's moment arm, will vary in proportion to the fibre cross-sectional area of the muscle. This approach assumes that muscles develop equal stress, minimizing the peak average stress developed within any one muscle of an agonist group. However, given that agonist muscle groups are typically composed of a heterogeneous distribution of muscle fibre types, the recruitment of motor units for muscle force generation often may be unevenly distributed among individual muscle agonists, so that this assumption must be treated cautiously.

Despite the assumptions (and limitations) inherent in the calculation of muscle forces using a non-invasive linked segment, free-body approach, changes in muscle force development can be usefully related to changes in muscle fibre length to estimate muscle power output (but see Chapter 4), as well as being used to calculate tendon strain energy storage and bone stress.

4.1 Muscle–tendon length changes

Changes in overall muscle–tendon length (dL_{tot}) are calculated from changes of joint angle ($d\theta$), in which $dL_{tot} = r_m\, d\theta$, for small $d\theta$. $d\theta$ may occur in two different planes, requiring a 3-D analysis of segmental motion. However, as noted above, motion of a limb or of a joint in many instances occurs within a single plane. In these cases, a planar analysis of joint motion is sufficient, greatly simplifying the complexity of the analysis involved. The remaining discussion considers a planar analysis of segment motion, in which the joint coordinate data are obtained from a lateral projection of the animal's limb.

To determine muscle length changes requires that changes in tendon length

('series elasticity') be subtracted from overall muscle–tendon length change. Knowledge of the changes in tendon length, in turn, requires that tendon strain (ε_{tend}) be determined (see below). Calculation of actual muscle fibre length changes within the muscle requires that the fibre architecture of the muscle is known.

4.2 Tendon strain, tendon strain energy, and muscle length change

Tendon strain and strain energy storage can be calculated knowing tendon elastic modulus (E), tendon cross-sectional area (A) and tendon volume (V). Tendon volume is most easily calculated from tendon mass, if the density of the tendon is known. Tendon density can be determined by Archimedes' principle (18), in which the piece of tendon is first weighed in air (as normally determined on an analytical balance) and subsequently re-weighed while immersed in a fluid (water) of known density. The density of the piece of tendon is given by

$$\rho_{tend} = \rho' \left[1 + \frac{W'}{W - W'}\right] \tag{14}$$

where ρ' is the density of the fluid, W is the weight of the tendon in air, and W' is the weight of the tendon while being hung fully immersed in the fluid. This method works quite well for objects (such as tendon) that are of similar density to water because errors in weight do not produce the same errors in density; rather, the error is with respect to the *difference* in density between the object and the fluid. A value of $1120\,kg\,m^{-3}$ has been reported for vertebrate tendon (25). Mean tendon cross-sectional area, then, is: $A = V/L$, where L is the length of the external tendon that is excised and weighed (it is critical that the tendon be weighed immediately to avoid desiccation; small tendons must be weighed to the nearest 0.1 mg). Alternatively, the cross-sectional area of larger tendons can be determined at specific sites along the tendon's length by cutting transversely through the tendon with a sharp scalpel and photographing the cut end of the tendon with a calibrated length measure in the camera's field. The photographs can then be magnified and digitized to determine local changes in tendon area (see Chapter 2). Once tendon area is determined, tendon stress is calculated as

$$\sigma_{tend} = F_{muscle}/A \tag{15}$$

yielding

$$\varepsilon_{tend} = \sigma_{tend}/E. \tag{16}$$

Tendon strain energy is calculated assuming that the average cross-sectional area of connective tissue contained *within* the muscle equals the mean A for the cut piece of tendon (that is, equal stress is assumed to be transmitted by

the collagen within the muscle to the collagen in the external tendon). This is done by treating the entire length of the tendon (L_{tend}) as passing from the muscle's point of origin to the tendon's insertion distally; so that tendon strain energy is

$$U_{tend} = 0.5 \cdot \sigma_{tend} \cdot \varepsilon_{tend} \cdot A \cdot L_{tend} \quad (17)$$

where $A \cdot L_{tend}$ is the total tendon volume strained by the force of the muscle. Finally, the length change of the muscle is

$$dL_{muscle} = dL_{tot} - (\varepsilon_{tend} \cdot L). \quad (18)$$

4.3 Muscle fibre area

The measurement of muscle fibre cross-sectional area is straightforward for parallel fibred muscles but less certain for pinnate muscles. Muscle volume is determined from muscle mass, based on a value for the density of muscle (vertebrate striated muscle generally has a density of 1060 kg m^{-3}; ref. 18). If there is reason to suspect a different density for the muscle of interest, the muscle's density can most easily be determined by Archimedes' principle (see above). For a parallel fibred muscle, muscle fibre area (A_{mus}) is simply muscle volume divided by the muscle's mean fibre length. For most parallel fibred muscles, fibre length does not vary much. However, in cases where muscle fibre length varies considerably throughout the muscle, carefully distributed measurements of muscle fibre length should be made to determine a mean fibre length. The use of a dissecting microscopic with a calibrated reticle in the eyepiece is especially useful for small muscles with short fibres (in the range of 2 to 20 mm). Otherwise, dial metric calipers can be used.

It should be noted that measurements of muscle fibre length are more accurately measurements of muscle *fascicle* length. At present, there is growing debate concerning the actual length of individual fibres within a muscle (see Chapter 8, Section 3). For many parallel fibred muscles, what appears to be a single 'fibre' running end to end within the muscle, actually may be several interdigitated fibres that taper and overlap in series with one another. This raises important questions with respect to the neural activation (fibre recruitment) of the muscle and details of force transmission within the muscle (between the actively contracting fibres and the connective tissue that binds them together). However, for the purposes of estimating a muscle's overall force generating potential or the average stress developed within the muscle, the issue of serially interdigitated shorter fibres is not a serious concern with respect to determining muscle fibre cross-sectional area.

For pinnately fibred muscles, the determination of muscle fibre area is complicated by the variable number of planes along which the fibres are angled, the variable length of the fibres within a plane and the variable angle of pinnation of the fibres. Typically, fibres change their angle of insertion on to the muscle's central tendon or sheath as one moves from the proximal to

more distal locations in the muscle. Consequently, a number of measurements of fibre length and pinnation angle distributed throughout the whole of the muscle are required to accurately sample the muscle. It is best to devise an objective scheme for sampling the muscle to achieve unbiased estimates of mean fibre length and pinnation angle. Knowledge of the muscle's internal architecture is also essential if it is to be sectioned properly for making measurements of fibre architecture.

Protocol 2 can be followed for making measurements of fibre geometry in both pinnate and parallel fibred muscles.

Protocol 2. Measurement of muscle fibre cross-sectional area

1. After being dissected free, the muscle should be carefully cleaned and weighed. At this point, muscle density can also be determined if necessary.
2. The muscle may be placed in a weak fixative (10% formalin) over night to improve the integrity of the tissue. However, formalin fixation causes shrinkage. This can be checked by comparing measurements of fibre length to those obtained from fresh tissue.
3. Using a sharp scalpel, the muscle should be cut transversely along its length *parallel* to the plane of an angled sheet of fibres within the muscle. If the muscle is multipinnate, then additional sections of the muscle must be made. This should be planned carefully, as making more than two or three sections often renders orientation of the muscle difficult. For small muscles, a dissecting microscope should be used.
4. Support the muscle so that the cut surface is level and facing upward. Cotton soaked in saline works well for this purpose. Ensure that the muscle approximates its 'resting' shape.
5. Sample and record muscle fibre length at standard intervals throughout the plane of section. Again, a dissecting microscope with a calibrated reticle is useful for very short fibres; however, in most instances a metric digital caliper works best.
6. Using a clear, lightweight protractor supported just over the surface of the muscle and a clear plastic ruler, measure angles of pinnation at the same locations where fibre length was determined. This measurement requires that the axis of the tendon of insertion (assumed to be the muscle's line of force transmission) be defined.[a]
7. After making measurements of muscle fibre length and angle on the fresh or mildly fixed muscle, muscle fibre length may be measured a second time, following acid digestion of the connective tissue to verify the original set of measurements. This procedure, however, precludes measurement of fibre angle. To carry out this procedure, immerse the muscle in 15% nitric

Protocol 2. *Continued*

acid and check after periods of 8, 16, and 24 hours, until individual muscle fibres can gently be freed from surrounding connective tissue using watchmaker's forceps. The lengths of individual muscle fibres can then be easily measured. Torn fibres are readily discerned from intact fibres by checking the ends under a dissecting microscope: torn fibres show abrupt tears or jagged ends in contrast to the slow taper of intact fibres.

[a] An alternative approach is to photograph the surface of the muscle and make the measurements of fibre length and fibre angle on the photographs. Though more time-consuming and costly, this step typically yields more accurate measurements. The values obtained from the photographed sections can be compared to the direct measurements to determine the necessity of this step.

The fibre area of a pinnate muscle can be calculated by the following equation given by Calow and Alexander (26):

$$A_{mus} = \frac{m \sin(2\alpha)}{2\,\rho_{mus}\, l \sin(\alpha)} \tag{19}$$

where m is the muscle's wet mass, ρ_{mus} is the muscle's density, l is the muscle's mean fibre length, and α is the mean pinnation angle. See ref. 26 for details concerning how the muscle's fibre geometry is modelled to derive the above equation.

4.4 Bone stress

Bone stresses are calculated by summing the net transverse (F_T), axial (F_A), and mediolateral (F_L) forces acting on the bone in question. In most cases, a planar analysis of bone stress is carried out in which either antero-posterior (A/P) or mediolateral forces are ignored, and no assessment of torsional loading or eccentric loading of the bone out of the plane of motion can be made. More commonly forces acting in the A/P plane are of interest (particularly for cursorial species that move their limbs in a para-sagittal plane) and mediolateral forces are ignored. Mediolateral forces must be considered, however, if a three-dimensional analysis of bone stress is required. The above components of force are generated by the combined effect of joint reaction forces transmitted by the ground reaction force, by muscular forces and by ligamentous forces, if present (*Figure 8*). The transverse and axial force component of each force vector are resolved in relation to the longitudinal axis of the bone (for example, for muscle force: $F_T$muscle $= F_{muscle} \cdot \sin\theta$; $F_A$muscle $= \cdot \cos\theta$). Axial compressive stress at the bone's midshaft then is

$$\sigma_A = -F_A/A_{bone} \tag{20}$$

where A_{bone} is the midshaft cortical cross-sectional area of the bone. Stress due to bending is

$$\sigma_B = \pm(F_T \cdot l + F_A \cdot r_{curv})\, c/I \tag{21}$$

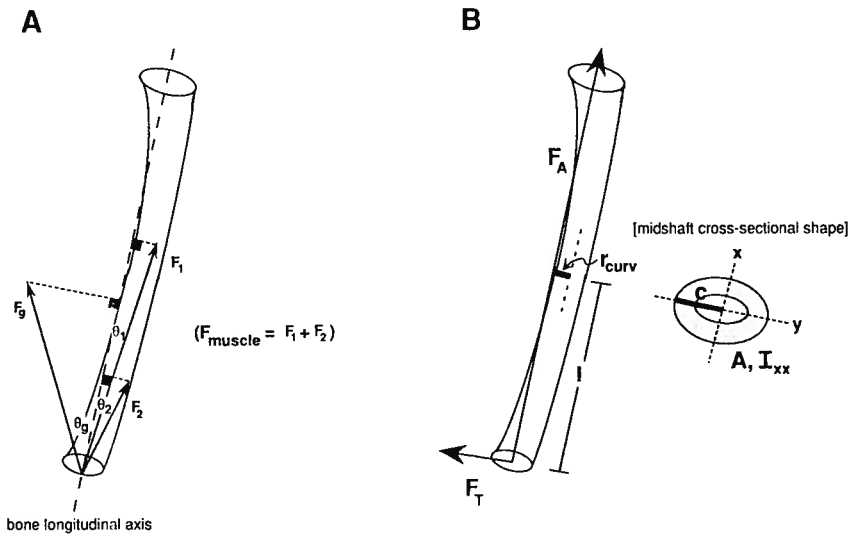

Figure 8. **A**: Free body diagram of the tibia, showing the axial and transverse components of each force vector relative to the bone's longitudinal axis (dashed lines). Axial components of force are determined by $F \cdot \cos\theta$ and transvere components by $F \cdot \sin\theta$. **B**: Net axial (F_A) and transverse (F_T) forces acting on the bone. In addition to the bending moment produced by F_T at the bone's midshaft ($=F_T \times l$), due to the bone's longitudinal curvature F_A also exerts a bending moment ($F_A \times r_{curv}$). Stresses due to axial compression (σ_c) and bending (σ_b) at the bone's midshaft are determined based on geometric properties of the bone's cortex at its midshaft (note that the calculations shown involve a planar analysis of the limb, limiting the computation of stresses to the antero-posterior plane, or the y-axis, of the bone).

where l is the distance from the articular surface of the bone to its midshaft, r_{curv} is the moment arm of the axial component of force acting about the bone's own longitudinal curvature in the plane of interest, c is the maximum distance from the neutral axis to the surface of the bone and I is the second moment of area of the bone at its midshaft (measured in the antero-posterior plane; see Chapters 1 and 2). For straight bones ($r_{curv} = 0$), no moment is exerted by F_A. The orientation of bending due to F_T and the bone's own curvature determines the distribution of stresses across the bone's cortex in the antero-posterior plane. Although r_{curv} is typically small in magnitude, the presence of longitudinal curvature in many long bones greatly affects the distribution of stresses developed across the bone's midshaft cortex (1, 5). Consequently, it is critical that it be measured accurately. r_{curv} in the A/P plane is best determined from a lateral radiograph of the bone, in which the longitudinal axis of the bone is established by the centres of rotation of the proximal and distal articular ends of the bone. r_{curv} is the distance from the longitudinal (chord) axis of the bone to the centroid of the bone's cross-

section. For fairly symmetric bones, the centroid may be assumed to be midway along the bone's diameter, making the measurement of r_{curv} more straightforward. Bone curvature and F_T are additive if F_T acts in the same direction as the concavity of the bone's curvature. For the case in which these are in the posterior direction of the bone's shaft, the stresses at the bone's anterior and posterior midshaft surfaces are respectively:

$$\sigma_{ant} = \sigma_A + \sigma_B; \quad \sigma_{post} = \sigma_A - \sigma_B \qquad (22, 23)$$

σ_{post} will be compressive (negative), and σ_{ant} will be tensile (positive) if σ_B exceeds σ_A.

This method provides a reasonably accurate means for determining the maximum stresses developed *generally* within a bone in a single plane. It is sensitive however to errors in measuring the magnitude of $F_T(l)$, which depends on the accuracy with which bone orientation to the ground reaction force and muscle vectors can be determined. Although the error may be small in terms of the absolute magnitude of F_T, because of a large value for l in long bones this can have a large effect on the calculation of stress due to bending at the bone's midshaft. In addition, this method provides little detail as to the distribution of stress or strain within the bone's shaft, which is exacerbated by ignoring out-of-plane forces. For this, *in vivo* measurements of surface bone strain (see Chapter 6) or finite element modelling methods (see Chapter 7) are necessary. *In vivo* measurements of bone strain can, in turn, be used to calculate or to verify the net components of axial and transverse force acting on the bone, based on an empirical value for the elastic modulus of bone which is needed to transform recorded strains to stresses (1).

The two important advantages of a combined force–kinematic analysis are that (i) it is non-invasive, minimizing concerns about the performance of the animal being studied, and (ii) it integrates estimates of bone stress and tendon stress (or strain) with the underlying muscle forces and ground reaction forces that must be generated to support and move the animal. Finally, this approach is crucial to establishing realistic values for the functional loads experienced by a bone element that are required for input to finite element models of the bone (see Chapter 7).

References

1. Biewener, A., Thomason, J. J., Goodship, A. E., and Lanyon, L. E. (1983). *J. Biomech.*, **16,** 565.
2. Kram, R. and Powell, A. (1989). *J. appl. Physiol.*, **67,** 1692.
3. Cavanagh, P. R. and LaFortune, M. A. (1980). *J. Biomech.*, **13,** 397.
4. Heglund, N. A. (1981). *J. exp. Biol.*, **93,** 333.
5. Biewener, A. A. (1983). *J. exp. Biol.*, **103,** 131.
6. Cavagna, G. A., Heglund, N. C., and Taylor, C. R. (1977). *Am. J. Physiol.*, **233,** R243.

7. Heglund, N. C., Cavagna, G. A., and Taylor, C. R. (1982). *J. exp. Biol.*, **79,** 41.
8. Full, R. F. and Tu, M. (1990). *J. exp. Biol.*, **148,** 129.
9. Winter, D. A. (1990). *Biomechanics and motor control of human movement.* John Wiley, New York.
10. Inoue, S. (1986). *Video microscopy*, p. 584. Plenum Press, New York.
11. Abdel-Aziz, Y. I. and Karara, H. M. (1971). Direct linear transformation from comparator coordinates into object space coordinates in close-range photogrammetry. American Society for Photogrammetry. Falls Church, VA.
12. Walton, J. S. (1981). *Proc. Int. Soc. Optical. Eng.*, **291,** 196.
13. Kuo, S. S. (1965). *Numerical methods and computers*, p. 234. Addison-Wesley, Reading, Massachusetts.
14. Miller, D. I. and Nelson, R. C. (1973). *Biomechanics of sport*, p. 246. Lea & Febiger, Philadelphia.
15. Winter, D. A., Sidwall, H. G., and Hobson, D. A. (1974). *J. Biomech.*, **7,** 157.
16. Zernicke, R. F., Caldwell, G., and Roberts, E. M. (1976). *Res. Q.*, **47(1),** 9.
17. Pezzack, J. C., Norman, R. W., and Winter, D. A. (1977). *J. Biomech.*, **10,** 377.
18. Alexander, R. McN. (1983). *Animal mechanics* (2nd edn). Blackwell Scientific Publications, London.
19. Wells, R. P. (1981). *Bull. Prosthet. Res.*, **18,** 15.
20. Schneider, K. and Zernicke, R. F. (1990). *Adv. Eng. Software*, **12,** 123.
21. Herzog, W. *J. Biomech.* (In press).
22. Pandy, M. G. and Zajac, F. E. (1991). *J. Biomech.*, **24,** 1.
23. Alexander, R. McN. (1974). *J. Zool., Lond.*, **173,** 549.
24. Biewener, A. A. (1983). *J. exp. Biol.*, **103,** 131.
25. Ker, R. F. (1981). *J. exp. Biol.*, **93,** 283.
26. Calow, L. J. and Alexander, R. McN. (1973). *J. Zool., Lond.*, **171,** 293.

Biomechanics—Structures and Systems

A Practical Approach

Edited by
A. A. BIEWENER

Department of Organismal Biology and Anatomy, The University of Chicago, Chicago, USA

OXFORD UNIVERSITY PRESS
—at—
OXFORD UNIVERSITY PRESS
Oxford New York Tokyo

Oxford University Press, Walton Street, Oxford OX2 6DP
Oxford New York Toronto
Delhi Bombay Calcutta Madras Karachi
Petaling Jaya Singapore Hong Kong Tokyo
Nairobi Dar es Salaam Cape Town
Melbourne Auckland
and associated companies in
Berlin Ibadan
Oxford is a trade mark of Oxford University Press

Published in the United States
by Oxford University Press, New York

A cataloguing record is available from the British Library on request

Library of Congress Cataloging in Publication Data
Biomechanics (structures and systems) : a practical approach / edited by A. A. Biewener.
p. cm. — (The Practical approach series)
Companion vol. to: Biomechanics (materials) / edited by J. F. Vincent.
Includes bibliographical references and index.
1. Biomechanics—Research—Methodology. I. Biewener, A. A. (Andrew A.) II. Biomechanics (materials) III. Series.
QP303.B5698 1992 591.1'852—dc20 91–40604
ISBN 0–19–963268–5
ISBN 0–19–963267–7 (p/b)

Set by Footnote Graphics, Warminster, Wilts
Printed in Great Britain by Information Press Ltd. Eynsham, Oxford

Preface

This book presents techniques and methods used to study a range of topics concerning the mechanical design and function of organisms at structural levels of their organization. In a companion volume (*Biomechanics—materials: a practical approach*, ed. J. F. Vincent, Oxford University Press), methods for investigating the mechanical properties of biomaterials are presented. Given the hierarchical and functionally integrative nature of organisms, studies of the mechanics of their structures must necessarily build on studies of the material properties of their tissues in order to understand how structural design yields higher level mechanical function. Consequently, some overlap between the two books is unavoidable. Questions of mechanical design and function, in turn, ultimately relate to organismal performance and the interaction of organisms with their physical environment. Much of this book focuses on musculoskeletal biomechanics, in which the design of muscular and skeletal elements is evaluated in the context of physical activities, such as running, flying, or feeding. Similarly, the mechanical design of circulatory systems (Chapter 10) concerns transport functions inside the organism related to carrying out these activities.

Although the main emphasis of the book is at an 'organismal' structural level, it should be noted that recent attempts to explore the biomechanics of cells and tissues make these promising areas of future research as well, particularly with regard to our understanding of mechanisms of signal transduction and the adaptive responses of biological tissues to mechanical stimuli. The book also maintains a strong comparative thread in most of the topics that are covered. It is hoped that for readers unfamiliar with the 'comparative method', the importance of this approach will emerge, not only for appreciating the intrinsic value of the organisms themselves, and their own phylogenetic history, but also in terms of its ability to discern basic patterns and principles of biological structure and mechanical function that have general application to other fields.

While the intent of the book is to present 'practical' approaches for studying the structural biomechanics of organisms, each chapter also includes conceptual and theoretical discussions as a background to the techniques and methods covered. In fact, in two of the chapters (Chapter 5, on the aerodynamics of flight; and Chapter 11, on the hydrodynamics of animal movement), concept and theory take precedence over technique. By doing so, our hope is to provide not only a useful 'guide' but also to convey some of the fascination, excitement, and importance of the topics that we study. The reader should recognize that most chapters serve only as a brief introduction to the techniques and methods presented. In many cases, additional reading